

# The role of heartwood water storage for sem-arid trees under drought

Guozheng Hu<sup>a,1</sup>, Hongyan Liu<sup>a,\*</sup>, Huailiang Shangguan<sup>a</sup>, Xiuchen Wu<sup>b</sup>, Xiaotian Xu<sup>a,2</sup>, Mathew Williams<sup>c</sup>

<sup>a</sup> Department of Ecology, College of Urban and Environmental Sciences, Peking University, Beijing 100871, China

<sup>b</sup> College of Resources Science and Technology, Beijing Normal University, Beijing 100875, China

<sup>c</sup> School of GeoScience, University of Edinburgh, Edinburgh, UK

## ARTICLE INFO

### Keywords:

Plant water pool  
Climate change  
Sap flow  
Dendrometer  
Heartwood water storage  
Water use strategy  
Water deficit  
*Populus*

## ABSTRACT

Stem water storage is an important water pool in forests. However, we know little about the heartwood water use processes and the water use strategies of trees in semi-arid temperate forests. We investigated Simon poplar (*Populus simonii*), a heartwood water storage tree species. A combination of methods (sap flow, the dendrometer and the soil–plant–atmosphere canopy model) were used to trace the water use dynamics of Simon poplar trees. The aim was to understand how this heartwood water storage tree species survives under drought stress.

Our field data showed that *P. simonii* had significantly higher heartwood water content (60%) than other tree species (30%) in the same region. The enhanced tree water deficit (TWD) and continuous stem shrinkage showed that the heartwood water supply was able to maintain sap flow (1.5–4.6 mm/d) during early growing season droughts. The strong water absorption ability of the roots resulted in the quick recovery of TWD, which caused the rain water could hardly reach 50 cm depth in the soil. The weakened link between transpiration and root water assimilation of heartwood water storage trees meant that sap flow was more sensitive to drivers such as air temperature ( $R = -0.71$ ,  $p < 0.01$ ) and vapor pressure deficit ( $R = 0.69$ ,  $p < 0.01$ ).

These results suggest that heartwood water storage may buffer drought events during the growing season and reduce the wide fluctuation in interannual precipitation. Therefore, heartwood water storage needs to be taken into account when calculating the soil–plant–atmosphere continuum and creating tree survival models.

## 1. Introduction

Recent global tree mortality and forest die off has been attributed to climate change; increases in the frequency, duration, and/or severity of drought; and heat stress (Barber et al., 2000, Klos et al., 2009, Allen et al., 2010, Dulamsuren et al., 2010, Choat et al., 2012, McDowell et al., 2016). Water stress during the growing season, caused by warming-induced increases in atmospheric moisture demand, has induced tree growth declines in the semi-arid forests of Inner Asia (Liu et al., 2013). Recent tree mortality has been observed in low-elevational temperate and southern boreal forest regions distributed close to the xeric tree line in Asia (Kharuk et al., 2013; Liu et al., 2013). Trees are a very important part of the soil–plant–atmosphere continuum (SPAC) in forest ecosystems because 60%–80% of terrestrial evapotranspirational water loss is directly controlled by plants (Schlesinger and Jasechko 2014). Therefore, the forest mortality risk can affect water cycling besides reduce the carbon sink process.

*Populus* species are widely distributed across the world and are known to be water-consuming species (Manzanera and Martínez-Chacón 2007, Beniwal et al., 2010). Simon poplar (*Populus simonii*) is one of the main species in the “Three-North Shelter Forest Program” (Zhang et al., 2016), which has been instigated in a semi-arid area close to the xeric tree line in China. Previous studies have shown that Simon poplar could maintain sap flow during the leaf-flushing period before useable precipitation had occurred (soil moisture < 8% above 1 m) (Hu et al., 2010) and during the dry growing season (soil moisture < 7% above 2 m) (Zhang et al., 2013).

Tree water use strategies focused on the response of stoma conduction (leaf transpiration, or leaf water potential) to soil drought (decrease of soil water content or potential) (McDowell et al., 2008, Parolari et al., 2014). Isohydric trees reduce stoma conduction as soil water potential decreases, while anisohydric species allow leaf transpiration as soil water potential declines with drought (McDowell et al., 2008). However, this hypothesis gives no explanation on the effect of

\* Corresponding author.

E-mail address: [lhy@urban.pku.edu.cn](mailto:lhy@urban.pku.edu.cn) (H. Liu).

<sup>1</sup> Present address: Institute of Environment and Sustainable Development in Agriculture, Chinese Academy of Agricultural Sciences, Beijing 100081, China.

<sup>2</sup> Present address: Research Institute of Desertification, Chinese Academy of Forestry, Beijing 100091, China.

tree water storage. Succulent trees, which store withdrawable water in living cells (Griffiths and Males, 2017), also have sensitive response of leaf to soil drought (De Smedt et al., 2012). However, rare studies focused on the effects of heartwood water storage in non-succulent trees on water use strategies, which may improve the isohydric hypothesis and provide widely adaptable implications for modelling research.

This study compared the water use dynamics of Simon poplars during growing season by taking field measurements and by using the soil–plant–atmosphere canopy model (SPA) where the water inputs were soil water from rainfall rather than stem water storage, because soil water is the main water source used in most stand-level models (Williams et al., 1996, Hanson et al., 2004). The water use process and soil dynamics of Simon poplars was also compared to two afforested coniferous species, larch (*Larix principis-rupprechtii*) and pine (*Pinus sylvestris* var. *mongolica*). We hypothesized that stem water storage may weaken the sensitivity of leaf transpiration to soil drought. The aims were to investigate (1) how stem water storage affects the transpiration process in the soil–plant–atmosphere continuum containing Simon poplar trees during drought, and (2) how Simon poplar trees use soil water. The results from this study could provide new information about forest responses to climate change, and improve our understanding of the water cycle process in the SPAC.

## 2. Materials and methods

### 2.1. Experimental site

Our experiment was located in the forest-steppe ecotone on the edge of the Otindag sandy land in southeastern Inner Mongolia, China (42°09'N; 116°17'E; 1350 m a.s.l. Fig. 1). Mean annual temperature (MAT) is 2.28 °C (1953–2013), which has significantly increased by 0.39 °C/10a ( $R^2 = 0.49$ ,  $p < 0.05$ ) during this period (Fig. S1). Mean annual precipitation is 364 mm (1953–2013), but annual precipitation

(AP) widely fluctuates and has not shown any significant trends between 1953 and 2013 (Fig. S2). Our experiment was carried out in afforested *Populus simonii*, *Larix principis-rupprechtii*, and *Pinus sylvestris* var. *mongolica* forests (Fig. S3). All the three investigated tree species were planted on similar stands with entisols, in which sand (grain size 0.063–2 mm) takes over 40% of the soil materials and roots were mostly distributed within the top 30 cm of the soil (Fig. S4). These afforested forests are parts of the “Three-North Shelter Forest Program”, which is a series of human-planted wind-shelter forest strips (shelterbelts) in North, Northeast, and Northwest China. A 20 m × 20 m plot was planted with Simon poplar, whereas 10 m × 10 m plots were used for the two needle leaf species as these two species were planted at a greater density than the Simon poplar (Table S1).

### 2.2. Meteorology

Air temperature ( $T_a$ ) and relative humidity (RH<sub>a</sub>) were measured and recorded with HOBO U23 pro v2 sensors (Onset Computer, Inc., Bourne, MA, USA). The device was placed at the bottom of the canopy on the north side of the stem to avoid direct sunlight. Precipitation data was recorded by a nearby weather station (Fig. 1). Shortwave radiation data was measured at Peking University Saihanbai Ecological Station (PKU station, Fig. 1), which was located at a similar altitude to our experimental site. Soil temperature and moisture were measured and recorded by an EM50 with TDR-type 5 TM sensors (Decagon Devices, Inc. Pullman, WA, USA). The sensors were placed at soil depths of 10, 30, 50, 100, and 150 cm. The temperature and moisture were interpolated each 10 cm soil layer down to 150 cm.

### 2.3. Sap flow measurement

Sap flow (SF, L/h) was measured in six trees per plot with SF-L (Ecomatik, Inc, Munich, Germany) Granier type thermal dissipation

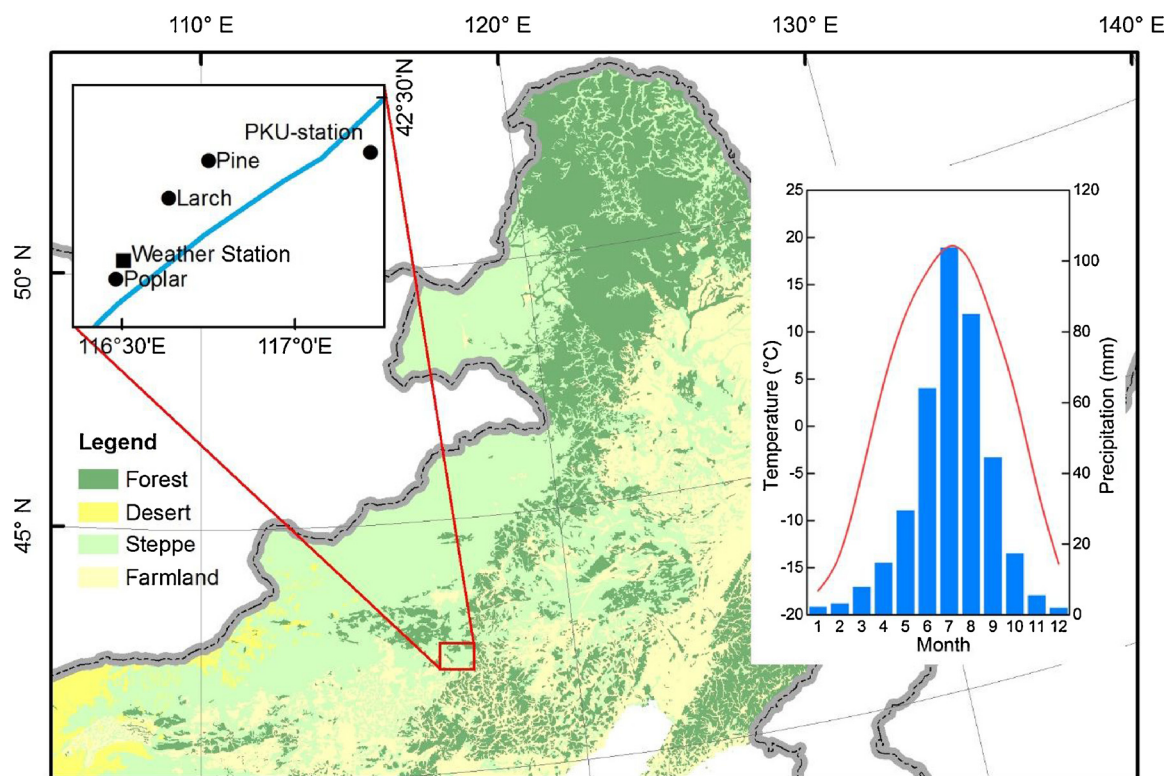


Fig. 1. The study area was located in the forest-steppe ecotone where there was a 400 mm precipitation isoline (blue line on the sites map) across the area. The study area had a typical continental climate and most precipitation occurred in summer (For interpretation of the references to colour in this figure legend, the reader is referred to the web version of this article).

probes (Granier 1987). The SF in each tree was measured every half hour throughout the day. The measurements were carried out during the growing season (May to September) in 2012 and 2013. They were measured on different days every two weeks for all three species in 2012 and for larch and pine in 2013 (Table S2). However, the Simon poplar SF was measured on continuous days in 2013 (Table S2).

The stand-scale SF (total sap flow per unit ground area, mm/h) was estimated from the tree-scale SF (Fisher et al., 2007). The sensors measured sap flux velocity (mL/cm<sup>2</sup>/min) and the SF of each tree equaled the sap flux velocity multiplied by the sapwood area, which was estimated from the wood core. A quadratic equation for diameter at breast height (DBH) was used to estimate the stand-scale SF, as sap flux velocity has been shown to be positively correlated with DBH (Fisher et al., 2007). The tree-scale SF (m/h) was estimated by

$$SF_{t,i} = (a_t \cdot d_i + b_t) \cdot d_i \quad (1)$$

where  $a_t$  and  $b_t$  were parameters at time  $t$ , and  $d_i$  was the DBH (cm) of the  $i$ th tree (Table S3). The stand-scale SF  $Q$  (mm/h) was then calculated as

$$Q_t = \frac{\sum_i SF_{t,i}}{A} \quad (2)$$

where  $A$  is the area of the plot (m<sup>2</sup>). As the scaling up relationship varied for each measured time, the calculation was batched in MATLAB 2016a (The MathWorks, Natick, Massachusetts, USA).

#### 2.4. Model description

The SPA model (see Williams et al., 1996 for a full description) was used to simulate the continuous sap flow in Simon poplar during the growing season because the continuous sap flow could be used to support any model adjustments. The SPA model is a multilayer soil–vegetation–atmosphere transfer (SVAT) model, in which changes in soil-to-root water supply can explain the transpiration response to soil drying (Williams et al., 1996, 1998, 2001). Most model parameters were defined by independent measurements at the experimental site (Table S4). Four parameters were adjusted in an attempt to best match predictions to the observed daily sap flow (Table S4). The adjustments were based on the original model parameterization as applied to temperate forests (Williams et al., 2000).

#### 2.5. Simulation protocol and meteorological drivers

Simulation started at April 1st (91 or 92 DOY) and ended at September 30th (273 or 274 DOY) each year. The sap flow data in 2013 were used to adjust the parameters because the data represented continuous measurements and the sap flow data for 2012 were used to test the model.

The inputs and drivers were mostly measured in this study (Table S5). Vapor pressure deficit (VPD) was calculated from the temperature and relative humidity data. Daily photosynthetically active radiation (PAR, MJ/m<sup>2</sup>/d) was simulated from the Bristow-Campbell model (Bristow and Campbell 1984):

$$\frac{R_G}{R_A} = a \cdot (1 - \exp(-b \cdot \Delta T^c)) \quad (3)$$

where  $R_G$  is PAR,  $R_A$  is extra-terrestrial solar radiation (MJ/m<sup>2</sup>/d),  $\Delta T$  is the daily temperature range (°C), and coefficients  $a$ ,  $b$ , and  $c$  were fitted using the short-wave radiation data from the PKU station (Fig. 1). Then the daily PAR data was interpolated for each hour (see Methods in supplementary information for details of PAR fitting and testing, Fig. S5).

#### 2.6. Stem growth and tree water deficit

The DBH variation was measured every half hour with DC type

dendrometers (Ecomatik). The devices were placed on the two trees that were also used for the SF measurements. The tree water deficit (TWD), which was first measured in 1975 (Hinckley and Bruckerhoff 1975), can be calculated from the dendrometer data, because stem shrinkage is most likely caused by water depletion in the stem. A “growth line” (or zero water stress line) was calculated from maximum value in the dendrometer data (Zweifel et al., 2005). Then, the TWD was calculated by subtracting the “growth line” from the dendrometer measurements (Zweifel et al., 2005). Thus, the TWD should be negative value, and the TWD enhanced when the value decreased. The daily maximum dendrometer data was used to eliminate the stem daily variation noise.

#### 2.7. Stem water content

Three tree ring samples were taken randomly and used to measure the stem water content. We took tree ring samples 10 times during the growing season. We also took samples from the two conifer species for comparison. The samples were divided into sapwood and heartwood and kept in ziplock bags. The fresh weight was measured within half an hour after sampling. The dry weight was measured after the samples were oven dried at 100 °C for 24 h. Then the stem water content was calculated from the dry and fresh weights.

#### 2.8. Time scaling of the data

Hourly data was used to compare the daily sap flow dynamic shown by the field measurements and the model simulation. Mean daily TWD was used to compare the tree water use dynamics with the modeled daily sap flow. Mean daily soil moisture data was used to compare the water source dynamics simulated by the SPA model for the growing season.

#### 2.9. Statistical analysis

The linear regression analysis between stem growth and accumulated precipitation was used to test the drought duration during the early growing season. Correlation coefficients between accumulated precipitation and lagged stem growth (from 0 to 40 days) were calculated for each tree. We also calculated the correlation between the model simulation and the field measurements to show the simulation effect of PAR (see supplemental data) and daily sap flow. The correlation coefficients between sap flow (at both the individual and stand-scale) and the atmospheric environmental factors (air temperature, relative humidity, and VPD) and the soil environmental factors (soil temperature and moisture at different depths) were calculated. The one-way analysis of variance (ANOVA) was carried out on the individual correlation coefficients between the three different afforested tree species. The paired-t test was used to analyze the differences in soil moisture between the model simulation and the field measurements, and the difference in water content between heartwood and sapwood for the different afforested species in this area.

### 3. Results

#### 3.1. Effect of environmental factors on stem growth dynamics

Air temperature and VPD were highly variable during the growing season (Fig. 2a and b). The precipitation varied throughout the long-term drought period during the early growing season (Fig. 2c and d). It was 295 mm during the growing season in 2012 and 381 mm in 2013, whereas the precipitation was only 38 mm from 90 to 160 DOY (April to June) in 2012 and 29 mm during the same period in 2013 (Fig. 2c and d). The dendrometer records showed that stem growth started at about 140 DOY (May) and ended at 210 DOY (July) in each year (Fig. 2c and d). The early growing season drought lasted 15 days in



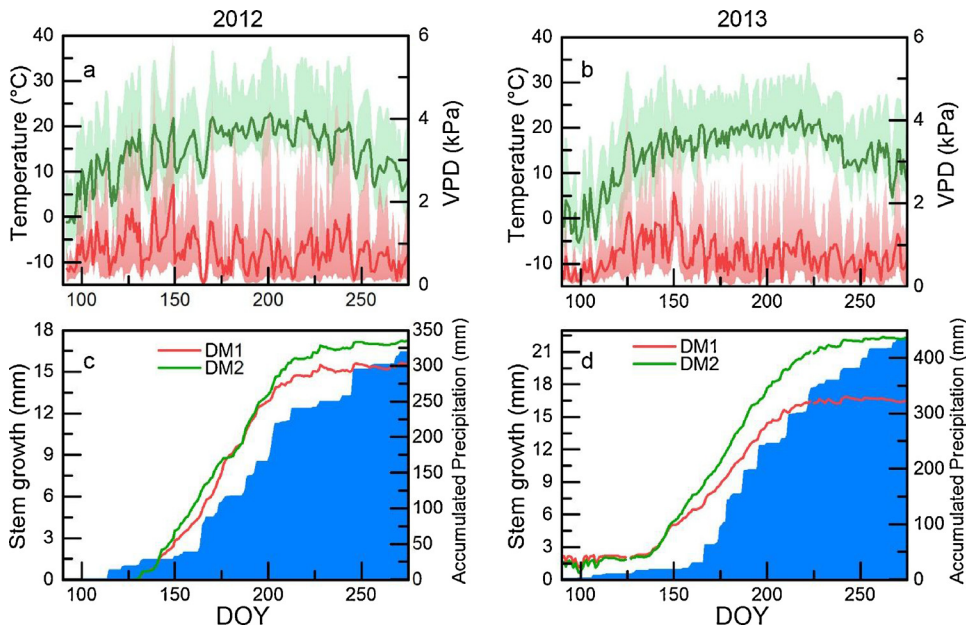


**Fig. 2.** Daily mean air temperature (green line) and VPD (red line) are shown along with the daily variation range from 90 to 250 DOY (April to September) in 2012 (a) and 2013 (b). The stem growth dynamics of two Simon poplar trees (red line for DM1, green line for DM2) are shown along with accumulated precipitation (blue area) from 90 to 250 DOY (April to September) in 2012 (c) and 2013 (d) (For interpretation of the references to colour in this figure legend, the reader is referred to the web version of this article).

2012 and 25 days in 2013 from the peak correlation coefficient between accumulated precipitation and lagged stem growth (Fig. S6).

The mean sapwood water content of Simon poplar was  $43.3 \pm 2.5\%$  and it was not significantly different from pine ( $43.2 \pm 2.6\%$ ) and larch ( $41.4 \pm 1.3\%$ ) (Fig. 3). However, the mean heartwood water content of Simon poplar was  $64.2 \pm 0.8\%$ , which was over two times more than the heartwood water content of pine ( $27.0 \pm 1.1\%$ ) and larch ( $31.7 \pm 1.2\%$ ) (Fig. 3).

### 3.2. Relationship between sap flow and environmental factors

The sap flow of the Simon poplars had different responses to environmental factors than the two other conifer species at both the stand-scale and tree-scale. The top three absolute correlation coefficients for the environmental factors and stand-scale sap flow for the Simon poplar forest were RHa (−0.59), Ta (−0.71), and VPD (0.69) (Table 1). About half of the soil environmental factors were not significantly correlated with stand-scale sap flow in the Simon poplars (Table 1). In contrast, soil environmental factors had the highest correlation coefficients with stand-scale sap flow in the larch and pine forests (Table 1).

### 3.3. Sap flow simulation of Simon poplar

The daily sap flow changed from 1.5 to 4.6 mm/d on sunny and

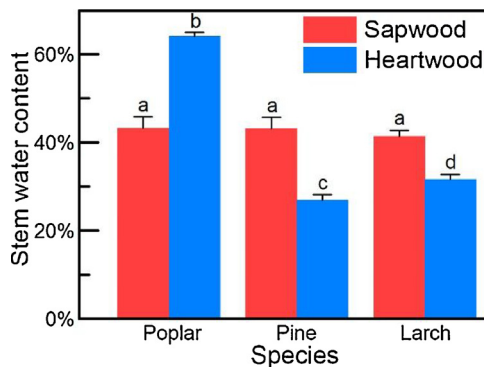


**Fig. 3.** Mean stem water contents of the sapwood and heartwood in the three afforestation species. Different letters indicate significantly different water contents between the samples ( $P < 0.05$ ).

**Table 1**

Correlation coefficients (R) with p values between the stand-scale sap flow and the environmental factors. Numbers in bold are the top three absolute correlation coefficients for environmental factors against stand-scale sap flow.

| Environmental factors | Poplar       |        | Larch       |        | Pine        |        |
|-----------------------|--------------|--------|-------------|--------|-------------|--------|
|                       | R            | p      | R           | p      | R           | p      |
| RHa                   | <b>−0.59</b> | < 0.01 | −0.22       | < 0.01 | −0.02       | 0.41   |
| Ta                    | <b>0.71</b>  | < 0.01 | <b>0.44</b> | < 0.01 | 0.17        | < 0.01 |
| VPD                   | <b>0.69</b>  | < 0.01 | 0.28        | < 0.01 | 0.01        | 0.43   |
| SM-10                 | −0.10        | < 0.01 | <b>0.40</b> | < 0.01 | 0.24        | < 0.01 |
| SM-30                 | 0.18         | < 0.01 | <b>0.37</b> | < 0.01 | 0.17        | < 0.01 |
| SM-50                 | 0.02         | 0.35   | 0.36        | < 0.01 | 0.32        | < 0.01 |
| SM-100                | 0.09         | < 0.01 | 0.28        | < 0.01 | <b>0.56</b> | < 0.01 |
| SM-150                | 0.05         | 0.10   | 0.29        | < 0.01 | 0.02        | 0.37   |
| ST-10                 | 0.14         | < 0.01 | 0.29        | < 0.01 | 0.10        | 0.06   |
| ST-30                 | 0.03         | 0.22   | 0.19        | < 0.01 | 0.28        | < 0.01 |
| ST-50                 | 0.10         | < 0.01 | 0.22        | < 0.01 | 0.38        | < 0.01 |
| ST-100                | 0.08         | < 0.05 | 0.16        | < 0.01 | <b>0.42</b> | < 0.01 |
| ST-150                | 0.05         | 0.11   | 0.13        | < 0.01 | <b>0.40</b> | < 0.01 |

cloudy days, respectively, and the daily sap flow stopped on rainy days (Fig. 4a, Fig. S8). The SPA model provided a good explanation for the changes in sap flow in 2013 (Fig. 4a, Fig. S7, & S8b) ( $R^2 = 0.63$ , slope = 0.69, intercept = 0.81 mm/d, RMSE (root-mean-square error) = 0.42 mm/d). However, the modeled sap flow was underestimated in 2012 (Figs. 4a & Figure 5b, Fig. S7). The sap flow was extremely underestimated on May 25th, August 24th, and September 22nd in 2012. The daily dynamic results showed that the modeled sap flow nearly stopped, whereas the sap flow actually continued on these days (Fig. 4).

### 3.4. Water use dynamics of Simon poplar trees

The water deficits of the two individual trees were mostly consistent during the growing season in 2012 (Fig. 5) and for the whole growing season in 2013 (Fig. S8). Only a small amount of precipitation occurred in the early part of the growing season, which caused that the TWD continued enhancing until the daily precipitation was over 30 mm at 165 DOY (June) in 2012 (Fig. 5) and 2013 (Fig. S8). However, it was virtually impossible to simulate sap flow during the dry early growing season before 160 DOY (June) in both years (Fig. 5b, Fig. S8b). The severest TWD occurred during 162–172 DOY (June) (Fig. 5a, Fig. S8a). The water use dynamics consistently showed that during the growing

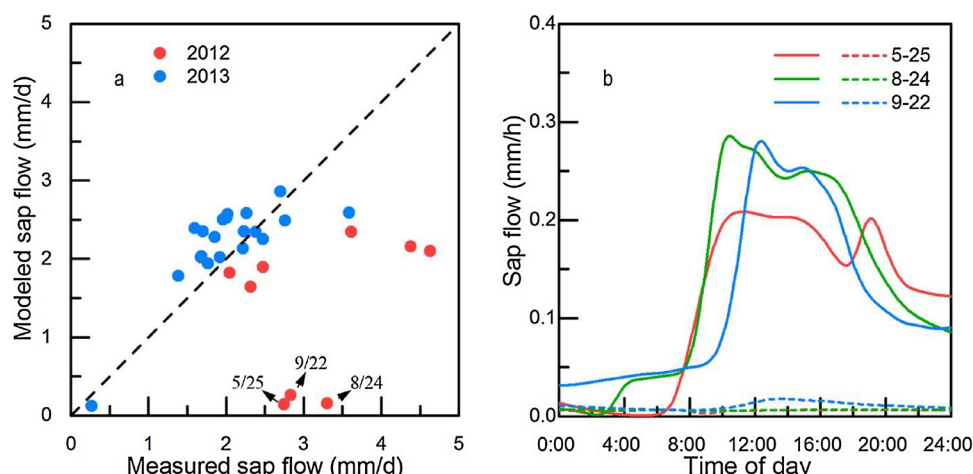


**Fig. 4.** Daily sap flow comparison between the modeled and measured data for Simon poplar in 2012 (a. red dot) and 2013 (a. blue dot). The dates of the three model outliers in 2012 are marked with arrows. (b) Comparison of the daily dynamics for sap flow between the modeled (dash line) and measured data (solid line) for the tree model outliers in 2012 (For interpretation of the references to colour in this figure legend, the reader is referred to the web version of this article).

season, the TWD strengthened during drier periods and lightened on rainy days (Fig. 5a, Fig. S8a). However, the modeled sap flow decreased during drier periods and recovered after rainy days (Fig. 5b, Fig. S8b).

### 3.5. Soil water dynamics

The soil water dynamics were different in the upper soil layers above 100 cm in the Simon poplar forest (Fig. 6a & S9a) than in SPA model (Fig. 6b & S9b), the larch (Fig. 6c & S9c) and pine (Fig. 6d & S9d) forests during the growing season. However, the soil water content was more stable in the Simon poplar forest according to the field measurements, and the rain only filtered down to 30 cm soil depth in 2012 and 2013 (Fig. 6a & S9a), but rain formed soil water pools developed according to the SPA model and at the two conifer sites. The rain could filter down to 70 cm depth soil in 2012 (Fig. 6b) and 110 cm in 2013 (Fig. S9b) in the Simon poplar forest according to the SPA model and the rain filtered down to over 50 cm depth soil in the larch and pine forests in both years (Fig. 6c, d & S9c, d).

The simulated soil moisture was 4.11% and 3.49% ( $p < 0.05$ ) higher at 10 cm and 30 cm depth than the field measurements in 2012, 3.33% and 3.65% ( $p < 0.05$ ) higher at 10 cm and 30 cm depth in 2013 (Fig. S10). The simulated soil moisture was 2.46% ( $p < 0.05$ ) lower at 50 cm depth in 2012 and 4.08% ( $p < 0.05$ ) lower in 2013 (Fig. S10). However, the pattern varied at 100 cm depth for the different years.

The simulated soil moisture was significantly lower in 2012 (Fig. S10a) and higher in 2013 (Fig. S10b) at 100 cm depth than the field measurements. At 150 cm, there were no significant differences between the field measurements and the simulation in 2012 (Fig. S10a), whereas the simulated soil moisture was significantly higher in 2013 (Fig. S10b).

## 4. Discussion

Heartwood water could be the direct transpiration source for water-storage trees. The TWD usually strengthens as the soil water potential decreases during dry periods (Zweifel et al., 2005; Vieira et al., 2013). However, in this study, the soil water potential remained stable when the soil moisture levels were low during early growing season in 2012 and 2013. Therefore, the strongly strengthened TWD indicated that there was insufficient water supply from the soil, but there was continuous heartwood water consumption during the early growing season, even though the SPA model showed that the soil could not provide enough water for transpiration when rainfall was low. This was consistent with reports that transpiration is maintained in different *Populus* species for 7 to 17 days after drought-stress (Braatne et al., 1992). Furthermore, stem water storage contributes 6%–28% of the daily water budget in subtropical trees (Laureano et al., 2015), which suggests that stem water storage is a direct water source during the growing season because the strengthened TWD was consistent with the

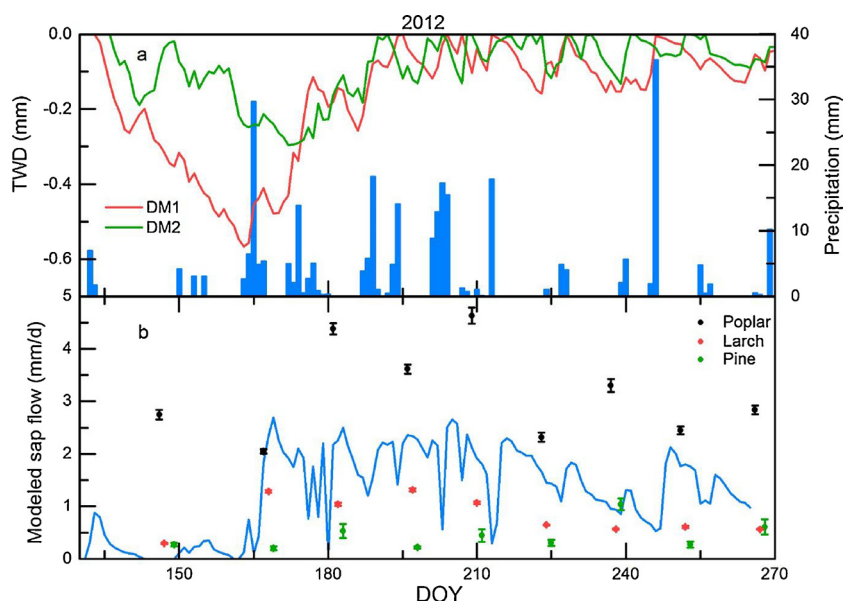


**Fig. 5.** (a). Tree water deficit dynamics are shown against daily precipitation in 2012. (b). Daily sap flow of Simon poplar (black point), larch (red point), and pine (green point) according to the field measurements and the continuous daily sap flow calculated using the SPA model (blue line) in 2012 (For interpretation of the references to colour in this figure legend, the reader is referred to the web version of this article).

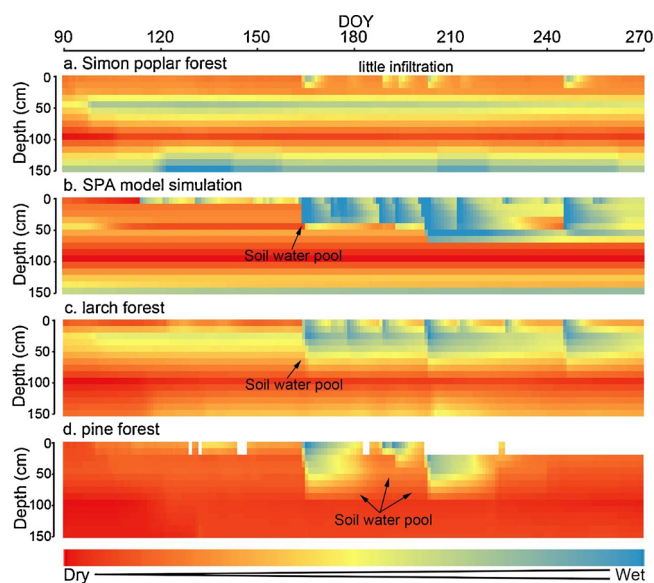


**Fig. 6.** The soil water dynamics were interpolated for each 10 cm soil layer from field measurements during the growing season in 2012 at the Simon poplar (a), larch (c), and pine (d) forests. (b) The soil water dynamics are compared to the SPA model simulation during the growing season in 2012. The red color represents 5% soil moisture whereas the blue color represents 15% soil moisture (For interpretation of the references to colour in this figure legend, the reader is referred to the web version of this article).

decrease in the simulated SF between two rainfall events in our study.

A potential pathway for water could exist between the heartwood and sapwood, as water movement between the heartwood and sapwood was reported in a deuterium-containing water injecting experiment (Kalma et al., 1998). Further evidence of heartwood water availability is that stem water contents change in the sapwood and heartwood (Wullschlegel et al., 1996). This study suggested that there was no direct radial pathway for water between the heartwood and sapwood and that the water content in the heartwood was significantly different to sapwood in each of the tree species investigated in our study. The water pathway consists of axial flows in the outer stem xylem because the radial pathway is blocked by the heartwood (Burgess and Bleby 2006; Nadezhdina et al., 2006). Although the radial pathway was supported by ray parenchyma between phloem and xylem (Pfautsch et al., 2015), water cannot transport between heartwood and sapwood with dead ray parenchyma. Therefore, we suggest that the roots are the most probable water link between heartwood and sapwood (a).

Water-storage trees may quickly assimilate water in the top soil layers and this may reduce infiltration into deeper soil layers (Fig. 7a). The stable soil moisture at 150 cm depth and the dry 100 cm depth soil could be the result of water absorption by the roots in the top layers (Fig. S4). The shallow, broad rooting systems take advantage of brief precipitation events (Ogburn and Edwards 2010), as rain events tend to be short in semiarid areas. The water from the upper soil layers has been shown to contribute to the transpiration of *Populus fremontii* during the summer rainy period (Snyder and Williams 2000). Simon poplars absorbed much more water than they transpired because the field measurements showed that much less water infiltrated the soil than was predicted by the SPA model when the daily sap flows were similar between the field data and the simulation. The strong tree absorption ability meant that the TWD lightened quickly after rainfall (Fig. 7a). Therefore, the Walter (1971) two-layer model needs to be modified when undertaking large scale modeling. Woody plants, as well as grasses, occupied water from the upper soil layer (Reynolds et al., 2000; Ward 2005; Wiegand et al., 2006; Rodríguez et al., 2007), although this hypothesis works remarkably well. In some cases, it is even appropriate for deserts, dry temperate systems, and some mesic

savannas (Ward et al., 2013).

The special water use strategy of water stored trees suggests that the heartwood water pool needs more consideration in SPAC and modeling studies (Sperry et al., 2003). The SPAC has become the predominant framework used for investigating the movement of water through plants (Goldsmith 2013). Previously, the tree stem has not been considered as a plant water pool (Fig. 7a), but as a pathway for water (Fig. 7b) in most stand-level forest ecosystem models (Hanson et al., 2004). Consequently, soil water was considered to be the main water source for trees, which meant that more water could infiltrate the deeper soil layers after heavy rain happened as in the soil moisture simulation by the SPA model (Fig. 7b non-water stored trees). However, heartwood water is an important water pool for trees and should not be ignored. Transpiration is often limited during soil drought, but may be maintained by stored water in the stem for about a week. However, it can only be maintained for a few hours by the water stored in the upper crown (Čermák et al., 2007), which was the main tree water storage area in the SPA model and other stand-level forest ecosystem models (Hanson et al., 2004). Furthermore, the stem can store water from both fog water uptake by foliar parts of the tree and soil water absorbed by the roots (Eller et al., 2013; Goldsmith 2013; Fu et al., 2016). A larger amount and steadier precipitation led to less severe TWD in 2013 than 2012. Therefore, less stem water storage was needed to compensate for the water deficiency and the soil water from precipitation infiltration was the main water source of transpiration in the SPA model in 2013. The SPA model thus performs better for 2013 than 2012.

Our study indicated that the tree water pool may weaken the link between transpiration and root water assimilation in water stored trees. The sap flow in the Simon poplar was more sensitive to the atmospheric driving factors (e.g.  $T_a$  and VPD) because water was supplied by large amounts of heartwood water storage rather than the soil, which limited sap flow in the larch and pine forests in our study area. This indicated that stoma conduction was not regulated by root signals, such as abscisic acid, during soil drought (Christmann et al., 2007). The sensitivity of root to soil drought may get weaken, if root link the water transportation from heartwood to sapwood. Therefore, heartwood water storage may buffer drought events during the growing season and the wide fluctuation in interannual precipitation. As the heartwood water storage support a drought tolerant strategy, it's hard to distinguish whether *P. simonii* is an anisohydric species or isohydric species with regards to heartwood water pool (McDowell et al., 2008). Contrarily, succulent trees always held an isohydric strategy and leaf shedding to avoid drought. Water storage in wood parenchyma attains its greatest expression, which formed a special morphological syndrome as pachycauly (Griffiths and Males, 2017). Stem water does not buffer daily water deficits for succulent trees during the rainy season (Chapotin et al., 2006b). Succulent trees used the stored water to initiate and almost entirely support leaf flush of new growth just prior to the start of the rainy season (Chapotin et al., 2006a; Griffiths and Males, 2017). And leaf shed at the beginning of the dry season as drought deciduous (Maes et al., 2009; Griffiths and Males, 2017). What's more, nocturnal carboxylation promoted competitive advantage of crassulacean acid metabolism (CAM) plants in arid environment (Yu et al., 2017a; Yu et al., 2017b), which is an integral component of the eco-physiology of the vast majority of succulents (Griffiths and Males, 2017). The identification of isohydric and anisohydric strategies from just the response of leaf water potential to soil water potential under drought condition needs to be reconsidered (McDowell et al., 2008). Further studies need to manipulate severe drought on mature heartwood water storage trees, which may reveal the isohydric or anisohydric strategies after the heartwood water deplete.

Heartwood water storage may play an important role in adaption to climate change as the frequency, duration, and/or severity of drought and heat stress increases. Early growing season droughts, induced by rapid warming in spring, decreases tree growth in the semi-arid mountain forests of Tianshan, northwest China (Wu et al., 2013). Our



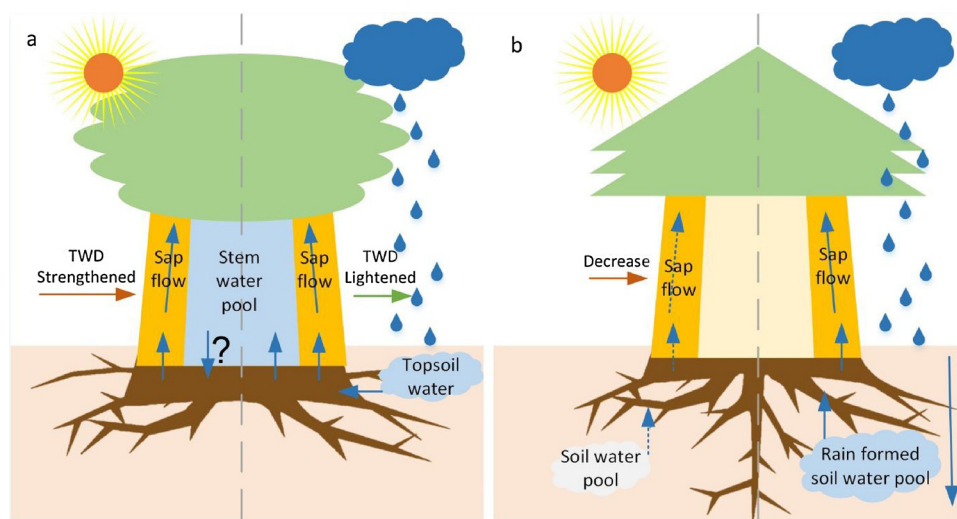


**Fig. 7.** The SPAC conceptual models for water stored trees (a) and non-water stored trees (b). Blue arrows represent the water flow in the soil and trees. During a drought between rain events, water stored trees can maintain sap flow by using the stem water pool, which enhances the tree water deficit (TWD) (a left). However, the sap flow of non-water stored trees is limited by the consumption of the soil water pool (b left). Water stored trees quickly assimilate topsoil water and more water is transferred to the stem water pool to lighten TWD on rainy days (a right). Precipitation is stored in the soil as a soil water pool in non-water stored trees sites, and more water infiltrates the deep soil layers when a large rain event occurs (b right) (For interpretation of the references to colour in this figure legend, the reader is referred to the web version of this article).

results showed that heartwood water storage supported transpiration, which enhanced the TWD when long drought events (about half a month) occurred during the growing season. Results from other models agree that northern East Asia, including Mongolia and north China, experienced a decrease in carbon storage from 1990 to 2009 and that this was caused by climate change (Piao et al., 2012).

## 5. Conclusions

The important contribution was revealed of heartwood water storage to transpiration. Simon poplar trees stored significantly higher water content (60%) in heartwood than other tree species (30%) in the same region. And this high heartwood water storage could induce higher sensitivity of sap flow to atmospheric driving factors, such as air temperature ( $R = -0.71$ ,  $p < 0.01$ ) and vapor pressure deficit ( $R = 0.69$ ,  $p < 0.01$ ), rather than the limited soil water. The dynamic of stem shrinking and recovering also indicated the compensative effects of heartwood water. The shrinkage during drought indicated that stem water storage supplied sap flow. The recovery of tree water deficit indicated that more water was assimilated than consumed by transpiration from soil. As root was suggested as the pathway between heartwood and sapwood, the sensitivity of root to soil drought may get weakened by heartwood water storage. Our results highlighted the importance of heartwood water storage in tree water use process, which provide new pointcut in SPAC and modelling studies. And that heartwood water storage tree species could be good choice for afforestation in the future.

## Acknowledgements

This research was funded by National Natural Science Foundation of China (NSFC No. 41325002 and 41530747). The research visit was founded by the short-term research exchange program of Peking University.

## Appendix A. Supplementary data

Supplementary material related to this article can be found, in the online version, at doi:<https://doi.org/10.1016/j.agrformet.2018.04.007>.

## References

- Allen, C.D., et al., 2010. A global overview of drought and heat-induced tree mortality reveals emerging climate change risks for forests. *For. Ecol. Manage.* 259 (4), 660–684.

- Barber, V.A., Juday, G.P., Finney, B.P., 2000. Reduced growth of Alaskan white spruce in the twentieth century from temperature-induced drought stress. *Nature* 405 (6787), 668–673.
- Beniwal, R.S., Langenfeld-Heyser, R., Polle, A., 2010. Ectomycorrhiza and hydrogel protect hybrid poplar from water deficit and unravel plastic responses of xylem anatomy. *Environ. Exp. Bot.* 69 (2), 189–197.
- Braatne, J.H., Hincley, T.M., Stettler, R.F., 1992. Influence of soil water on the physiological and morphological components of plant water balance in *Populus trichocarpa*, *Populus deltoides* and their F1 hybrids. *Tree Physiol.* 11 (4), 325–339.
- Bristow, K.L., Campbell, G.S., 1984. On the relationship between incoming solar radiation and daily maximum and minimum temperature. *Agric. Forest Meteorol.* 31 (2), 159–166.
- Burgess, S., Bleby, T., 2006. Redistribution of soil water by lateral roots mediated by stem tissues. *J. Exp. Bot.* 57 (12), 3283–3291.
- Čermák, J., Kučera, J., Bauerle, W.L., Phillips, N., Hincley, T.M., 2007. Tree water storage and its diurnal dynamics related to sap flow and changes in stem volume in old-growth Douglas-fir trees. *Tree Physiol.* 27 (2), 181–198.
- Chapotin, S.M., Razanameharizaka, J.H., Holbrook, N.M., 2006a. Baobab trees (*Adansonia*) in Madagascar use stored water to flush new leaves but not to support stomatal opening before the rainy season. *New Phytol.* 169 (3), 549–559.
- Chapotin, S.M., Razanameharizaka, J.H., Holbrook, N.M., 2006b. Water relations of baobab trees (*Adansonia* spp. L.) during the rainy season: does stem water buffer daily water deficits? *Plant Cell Environ.* 29 (6), 1021–1032.
- Choat, B., et al., 2012. Global convergence in the vulnerability of forests to drought. *Nature* 491 (7426), 752–755.
- Christmann, A., Weiler, E.W., Steudle, E., Grill, E., 2007. A hydraulic signal in root-to-shoot signalling of water shortage. *Plant. J.* 52 (1), 167–174.
- De Smedt, S., et al., 2012. Functional responses of baobab (*Adansonia digitata* L.) seedlings to drought conditions: differences between western and south-eastern Africa. *Environ. Exp. Bot.* 75, 181–187.
- Dulamsuren, C., Hauck, M., Leuschner, C., 2010. Recent drought stress leads to growth reductions in *Larix sibirica* in the western Khentey. *Mong. Global Change Biol.* 16 (11), 3024–3035.
- Eller, C.B., Lima, A.L., Oliveira, R.S., 2013. Foliar uptake of fog water and transport belowground alleviates drought effects in the cloud forest tree species, *Drimys brasiliensis* (Winteraceae). *New Phytol.* 199 (1), 151–162.
- Fisher, R.A., et al., 2007. The response of an Eastern Amazonian rain forest to drought stress: results and modelling analyses from a throughfall exclusion experiment. *Glob. Change Biol.* 13 (11), 2361–2378.
- Fu, P.-L., Liu, W.-J., Fan, Z.-X., Cao, K.-F., 2016. Is fog an important water source for woody plants in an Asian tropical karst forest during the dry season? *Ecophysiology* 9 (6), 964–972.
- Goldsmith, G.R., 2013. Changing directions: the atmosphere–plant–soil continuum. *New Phytol.* 199 (1), 4–6.
- Granier, A., 1987. Evaluation of transpiration in a Douglas-fir stand by means of sap flow measurements. *Tree Physiol.* 3 (4), 309–320.
- Griffiths, H., Males, J., 2017. Succulent plants. *Curr. Biol.* 27 (17), R890–R896.
- Hanson, P.J., et al., 2004. Oak forest carbon and water simulations: model inter-comparisons and evaluations against independent data. *Ecol. Monogr.* 74 (3), 443–489.
- Hincley, T.M., Bruckerhoff, D.N., 1975. The effects of drought on water relations and stem shrinkage of *Quercus alba*. *Can. J. Bot.* 53 (1), 62–72.
- Hu, W., et al., 2010. Analysis on sap flow of populus davidiana plantation in the leaf-flushing period in hilly-gully region of loess plateau. *J. Soil Water Conserv.* 24 (04), 48–52 (in Chinese with English abstract).
- Kalma, S.J., Thornburn, P.J., Dunn, G.M., 1998. A comparison of heat pulse and deuterium tracing techniques for estimating sap flow in *Eucalyptus grandis* trees. *Tree Physiol.* 18 (10), 697–705.
- Kharuk, V.I., Im, S.T., Oskorbin, P.A., Petrov, I.A., Ranson, K.J., 2013. Siberian pine

- decline and mortality in southern siberian mountains. *For. Ecol. Manage.* 310, 312–320.
- Klos, R.J., Wang, G.G., Bauerle, W.L., Rieck, J.R., 2009. Drought impact on forest growth and mortality in the southeast USA: an analysis using Forest health and monitoring data. *Ecol. Appl.* 19 (3), 699–708.
- Laureano, O.C., et al., 2015. Water storage dynamics in the main stem of subtropical tree species differing in wood density, growth rate and life history traits. *Tree Physiol.* 35 (4), 354–365.
- Liu, H., et al., 2013. Rapid warming accelerates tree growth decline in semi-arid forests of Inner Asia. *Glob. Change Biol.* 19 (8), 2500–2510.
- Maes, W.H., et al., 2009. Plant–water relationships and growth strategies of *Jatropha curcas* L. seedlings under different levels of drought stress. *J. Arid Environ.* 73 (10), 877–884.
- Manzanera, J.A., Martínez-Chacón, M.F., 2007. Ecophysiological competence of *populus alba* L., *fraxinus angustifolia* vahl., and *crataegus monogyna* jacq. used in plantations for the recovery of riparian vegetation. *Environ. Manage.* 40 (6), 902–912.
- McDowell, N., et al., 2008. Mechanisms of plant survival and mortality during drought: why do some plants survive while others succumb to drought? *New Phytol.* 178 (4), 719–739.
- McDowell, N.G., et al., 2016. Multi-scale predictions of massive conifer mortality due to chronic temperature rise. *Nat. Clim. Change* 6 (3), 295–300.
- Nadezhdina, N., Čermák, J., Gašpárek, J., Nadezhdin, V., Prax, A., 2006. Vertical and horizontal water redistribution in Norway spruce (*Picea abies*) roots in the Moravian Upland. *Tree Physiol.* 26 (10), 1277–1288.
- Ogburn, R.M., Edwards, E.J., 2010. The ecological water-use strategies of succulent plants. Chapter 4 In: Jean-Claude, K., Michel, D. (Eds.), *Advances in Botanical Research*. Academic Press, pp. 179–225.
- Parolari, A.J., Katul, G.G., Porporato, A., 2014. An ecohydrological perspective on drought-induced forest mortality. *J. Geophys. Res.: Biogeosci.* 119 (5), 965–981.
- Pfautsch, S., Renard, J., Tjoelker, M.G., Salih, A., 2015. Phloem as capacitor: radial transfer of Water into Xylem of tree stems occurs via symplastic transport in ray Parenchyma. *Plant Physiol.* 167 (3), 963–971.
- Piao, S., et al., 2012. The carbon budget of terrestrial ecosystems in East Asia over the last two decades. *Biogeosciences* 9 (9), 3571–3586.
- Reynolds, J.F., Kemp, P.R., Tenhunen, J.D., 2000. Effects of long-term rainfall variability on evapotranspiration and soil water distribution in the Chihuahuan Desert: a modeling analysis. *Plant Ecol.* 150 (1), 145–159.
- Rodríguez, M.V., Bertiller, M.B., Bisigato, A., 2007. Are fine roots of both shrubs and perennial grasses able to occupy the upper soil layer? A case study in the arid Patagonian Monte with non-seasonal precipitation. *Plant Soil* 300 (1), 281–288.
- Schlesinger, W.H., Jasechko, S., 2014. Transpiration in the global water cycle. *Agric. For. Meteorol.* 189–190, 115–117.
- Snyder, K.A., Williams, D.G., 2000. Water sources used by riparian trees varies among stream types on the San Pedro River, Arizona. *Agric. Forest Meteorol.* 105 (1–3), 227–240.
- Sperry, J.S., Stiller, V., Hacke, U.G., 2003. Xylem hydraulics and the soil–plant–atmosphere continuum. *Agron. J.* 95 (6), 1362–1370.
- Vieira, J., Rossi, S., Campelo, F., Freitas, H., Nabais, C., 2013. Seasonal and daily cycles of stem radial variation of *Pinus pinaster* in a drought-prone environment. *Agric. Forest Meteorol.* 180, 173–181.
- Walter, H., 1971. Natural Savannas as a Transition to the Arid Zone. *Ecology of Tropical and Subtropical Vegetation*. Oliver and Boyd, Edinburgh, pp. 238–265.
- Ward, D., 2005. Do we understand the causes of bush encroachment in African savannas? *Afr. J. Range Forage Sci.* 22 (2), 101–105.
- Ward, D., Wiegand, K., Getzin, S., 2013. Walter's two-layer hypothesis revisited: back to the roots!. *Oecologia* 172 (3), 617–630.
- Wiegand, K., Saltz, D., Ward, D., 2006. A patch-dynamics approach to savanna dynamics and woody plant encroachment – insights from an arid savanna. *Perspect. Plant Ecol. Evol. System.* 7 (4), 229–242.
- Williams, M., Eugster, W., Rastetter, E.B., McFadden, J.P., Chapin Iii, F.S., 2000. The controls on net ecosystem productivity along an Arctic transect: a model comparison with flux measurements. *Global Change Biology* 6 (S1), 116–126.
- Williams, M., Law, B.E., Anthoni, P.M., Unsworth, M.H., 2001. Use of a simulation model and ecosystem flux data to examine carbon–water interactions in ponderosa pine. *Tree Physiol.* 21 (5), 287–298.
- Williams, M., et al., 1998. Seasonal variation in net carbon exchange and evapotranspiration in a Brazilian rain forest: a modelling analysis. *Plant Cell Environ.* 21 (10), 953–968.
- Williams, M., et al., 1996. Modelling the soil–plant–atmosphere continuum in a *Quercus–Acer* stand at Harvard Forest: the regulation of stomatal conductance by light, nitrogen and soil/plant hydraulic properties. *Plant Cell Environ.* 19 (8), 911–927.
- Wu, X., Liu, H., Wang, Y., Deng, M., 2013. Prolonged limitation of tree growth due to warmer spring in semi-arid mountain forests of Tianshan, northwest China. *Environ. Res. Lett.* 8 (2), 024016.
- Wullschlegel, S.D., Hanson, P.J., Todd, D.E., 1996. Measuring stem water content in four deciduous hardwoods with a time-domain reflectometer. *Tree Physiol.* 16 (10), 809–815.
- Yu, K., D'Odorico, P., Carr, D.E., Personius, A., Collins, S.L., 2017a. The effect of nitrogen availability and water conditions on competition between a facultative CAM plant and an invasive grass. *Ecol. Evol.* 7 (19), 7739–7749.
- Yu, K., D'Odorico, P., Li, W., He, Y., 2017b. Effects of competition on induction of crassulacean acid metabolism in a facultative CAM plant. *Oecologia* 184 (2), 351–361.
- Zhang, J., et al., 2013. Soil water regime in *populus euphratica* forest on the tarim river alluvial plain. *Acta Phytocologica Sinica* 33 (18), 5655–5660 (in Chinese with English abstract).
- Zhang, X., et al., 2016. Three-North Shelter Forest Program contribution to long-term increasing trends of biogenic isoprene emissions in northern China. *Atherosclerosis (Amsterdam, Netherlands)* 16 (11), 6949–6960.
- Zweifel, R., Zimmermann, L., Newbery, D.M., 2005. Modeling tree water deficit from microclimate: an approach to quantifying drought stress. *Tree Physiol.* 25 (2), 147–156.